JACS
JOURNAL OF THE AMERICAN CHEMICAL SOCIETY
pubs.acs.org/JACS
Communication

The Application of Pulse Radiolysis to the Study of Ni(I) Intermediates in Ni-Catalyzed Cross-Coupling Reactions

Nicholas A. Till, Seokjoon Oh, David W. C. MacMillan,* and Matthew J. Bird*

Cite This: https://doi.org/10.1021/jacs.1c04652
Read Online
ACCESS | Metrics & More | Article Recommendations | Supporting Information

ABSTRACT: Here we report the use of pulse radiolysis and spectroelectrochemistry to generate low-valent nickel intermediates relevant to synthetically important Ni-catalyzed cross-coupling reactions and interrogate their reactivities toward comproportionation and oxidative addition processes. Pulse radiolysis provided a direct means to generate singly reduced [(dtbbpy)NiBr], enabling the identification of a rapid Ni(0)/Ni(II) comproportionation process taking place under synthetically relevant electrolysis conditions. This approach also permitted the direct measurement of Ni(I) oxidative addition rates with electronically differentiated aryl iodide electrophiles (k_{OA} = 1.3 × 10^4–2.4 × 10^5 M^{-1} s^{-1}), an elementary organometallic step often proposed in nickel-catalyzed cross-coupling reactions. Together, these results hold implications for a number of Ni-catalyzed cross-coupling processes.

Over the past 10 years, significant advances in nickel-mediated cross-coupling technology have elevated this mode of catalytic bond formation to widespread use in both academic and industrial settings.[1,2] At the same time, the development of dual-catalytic Ni/photoredox[3−5] and Ni/electrocatalysis[6−8] platforms, as well as further developments in Zn- and Mn-mediated reductive coupling reactions,[9] has enabled a wide array of challenging and/or unique C−C and C−heteroatom couplings that were previously unknown. In practice, these advances have led to the wide-scale adoption of nickel cross-coupling reactions across many industrial sectors, perhaps most notably the medicinal chemistry community.[10,11] While the development and deployment of these technologies has taken place at an impressive rate, a detailed understanding of the underlying mechanisms responsible for these new bond-forming processes has lagged behind in comparison.[12]

The use of photoredox and electrocatalysis has proven particularly valuable in modulating nickel oxidation states and generating transient high-energy radical intermediates that, in turn, can readily participate in previously elusive bond-forming processes.[6,13,14] While such reaction pathways provide a means to forge otherwise challenging C−C and C−heteroatom bonds, the fleeting nature of these catalytic Ni species makes them accordingly difficult to study. Electroanalytical techniques, such as cyclic voltammetry, can be used to probe the propensity for catalyst oxidation and reduction as well as the fate of resulting electrogenerated transition metal intermediates. For dual-catalytic Ni/photoredox reactions, Stern−Volmer quenching experiments are routinely utilized to measure rapid photoinduced electron-transfer rates, and transient absorption spectroscopy can provide insight into ensuing elementary steps.[15−21] However, while electroanalytical[22−25] and spectroscopic techniques have provided invaluable insight into many open-shell processes, the use of these experiments is less informative for reactions involving intermediates that exhibit non-reversible redox behavior or which participate in low quantum efficiency steps. Moreover,

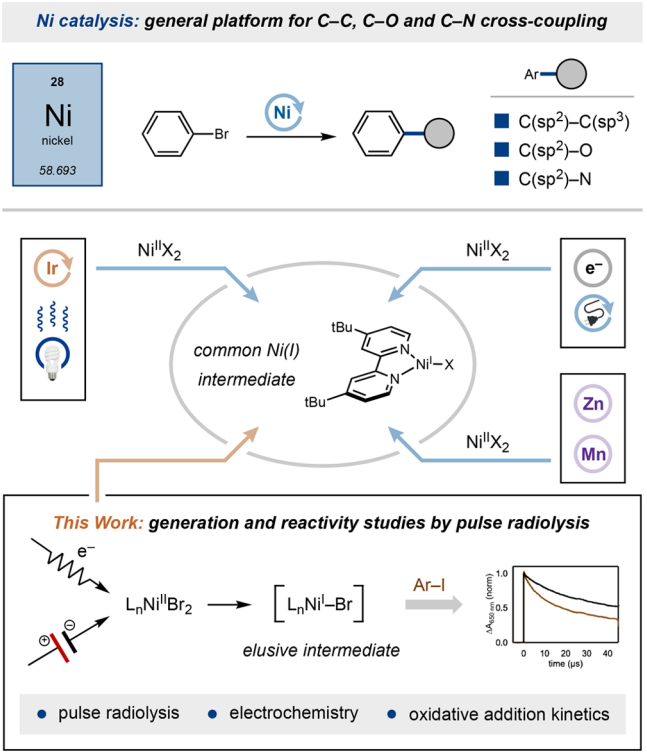

Figure 1. Approach to studying elusive Ni(I) intermediates.

Received: May 4, 2021

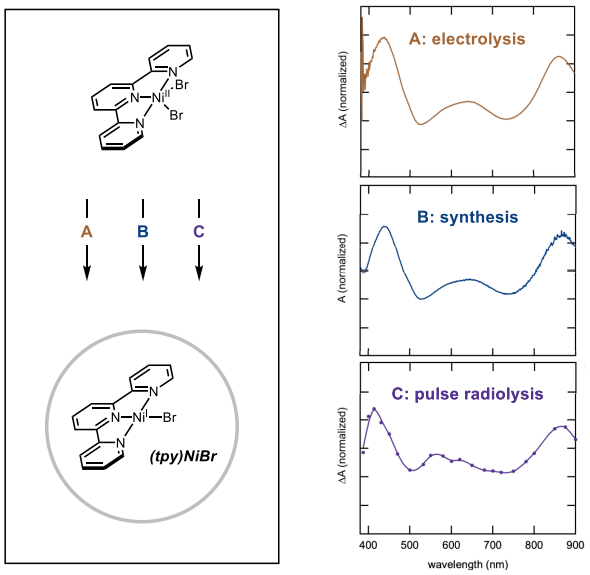

Figure 2. Normalized $\Delta A/A$ data for [(tpy)NiBr] generated by electrolysis (E_{app} = −750 mV vs SCE) (A), stoichiometric synthesis (B), and pulse radiolysis (t = 100 ns) (C).

multiple recent observations of radical chain mechanisms involving photogenerated Ni(I)/Ni(III) species further underscore the need to examine catalytic intermediates produced with low quantum yields that nonetheless are responsible for significant levels of product formation.[16,17,19]

While significant mechanistic complexity is a hallmark of nickel-catalyzed cross-coupling reactions, initial single-electron reduction of the employed Ni(II) dihalide precatalyst is a commonly proposed initiation event across many of these transformations (Figure 1).[12,16,26−28] The relative instability of the corresponding three-coordinate Ni(I) halide complexes resulting from reduction of the respective Ni(II) precatalyst makes studying these catalytic intermediates challenging. Such Ni(I) complexes can be generated with sterically encumbered ligands;[29−31] however, the cross-coupling relevant bipyridine-ligated analogs form stable and unreactive halide-bridged dimers or Ni(I)−Ni(II) mixed-valent bimetallic species.[16,20,32] For these reasons, the study of catalytically active, coordinatively unsaturated Ni(I) intermediates has remained largely unexplored.

Pulse radiolysis has a rich history of successfully probing reactivities of short-lived catalytic intermediates,[33,34] interrogating biological redox reactions,[35] and measuring fast electron-transfer rates.[36] Enabled by MeV electron pulses, this technique induces rapid solvent ionization, followed by electron or hole transfer to the solute of interest. When coupled to an appropriate light source and detector, time-resolved optical absorption measurements can be made on the transiently generated oxidized or reduced intermediates.[37] Importantly, the judicious choice of an appropriate organic solvent can ensure the selective generation of solvated electrons, thereby providing access to short-lived reduced intermediates in a catalytically relevant setting. Pulse radiolysis is particularly well-suited to studying short-lived Ni(I) intermediates, as the rapid injection of a low concentration of charges enables (i) selective one-electron reduction, (ii) generation of monomeric intermediates, and (iii) time-resolved measurements of ns−μs time scale follow-on reactions. Given these parameters, we were optimistic that pulse radiolysis could

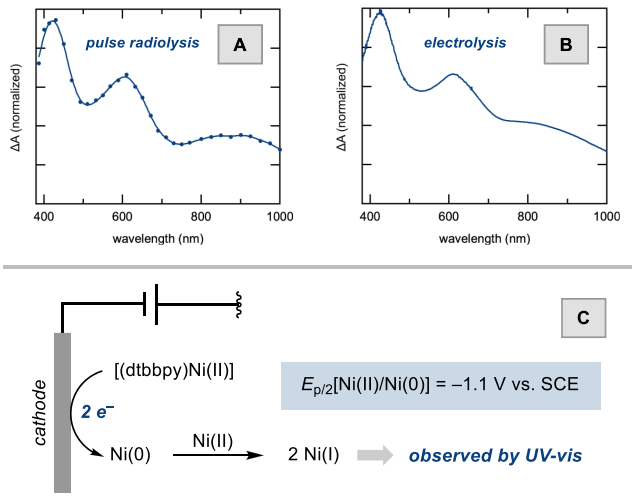

Figure 3. Normalized ΔA data for [(dtbbpy)NiBr] generated by pulse radiolysis (see SI, pages S4 and S16, for details) (A), ΔA data obtained upon electrolysis of [(dtbbpy)$NiBr_2$] (B), and the proposed mechanism of electrolytic Ni(I) generation (C).

be used to generate highly reactive Ni(I) species relevant to recently developed Ni-catalyzed cross-coupling reactions. If successful, the outlined approach would provide a platform for undertaking a wide range of reactivity studies with short-lived Ni(I) intermediates which would otherwise be difficult to study.

To initiate our study of transiently generated Ni(I) intermediates, we first turned our attention to validating the use of pulse radiolysis to generate the proposed Ni(I) bipyridine species. To this end, terpyridine-ligated Ni(I) bromide, previously reported by Vicic and co-workers,[38] was employed as a model system. Because this four-coordinate Ni(I) complex is sufficiently stable to permit traditional stoichiometric organometallic studies,[39] we reasoned that independent synthesis and spectroelectrochemical generation could serve as a means to verify putative Ni(I) signals generated by reductive pulse radiolysis of the corresponding terpyridine-ligated Ni(II)Br_2 precursor, [(tpy)$NiBr_2$] (tpy = 2,2′:6′,2″-terpyridine). For these measurements, *N*,*N*-dimethylformamide (DMF) was selected as an optimal solvent, as it is commonly employed in Ni-catalyzed cross-coupling reactions[9,13,28] and generates solvated electrons upon pulse radiolytic ionization (Figure S11).[40] Spectroelectrochemical measurements with a solution of [(tpy)$NiBr_2$] in DMF showed pronounced differences in absorption features (ΔA post-electrolysis vs pre-electrolysis, Figures 2A and S29) at 430, 600, and 860 nm, which align well with the analogous absorbance spectrum obtained from a synthetic sample of [(tpy)NiBr] (Figure 2B). Using the 9 MeV Laser Electron Accelerator Facility (LEAF),[37] a solution of [(tpy)$NiBr_2$] (20 mM in DMF) was then irradiated under pulse radiolytic conditions (see Supporting Information (SI), pages S4 and S16, for details), generating ΔA features mirroring those observed under electrolytic and synthetic conditions (Figure 2C), validating the use of pulse radiolysis to generate and spectroscopically investigate Ni(I) intermediates.

The electrochemical reduction of [(dtbbpy)$NiBr_2$] (dtbbpy = 4,4′-di-*tert*-butyl-2,2′-bipyridine) is irreversible by cyclic voltammetry at moderate scan rates (100 mV/s, Figure S33), and previous studies have revealed that the corresponding

https://doi.org/10.1021/jacs.1c04652
J. Am. Chem. Soc. XXXX, XXX, XXX−XXX

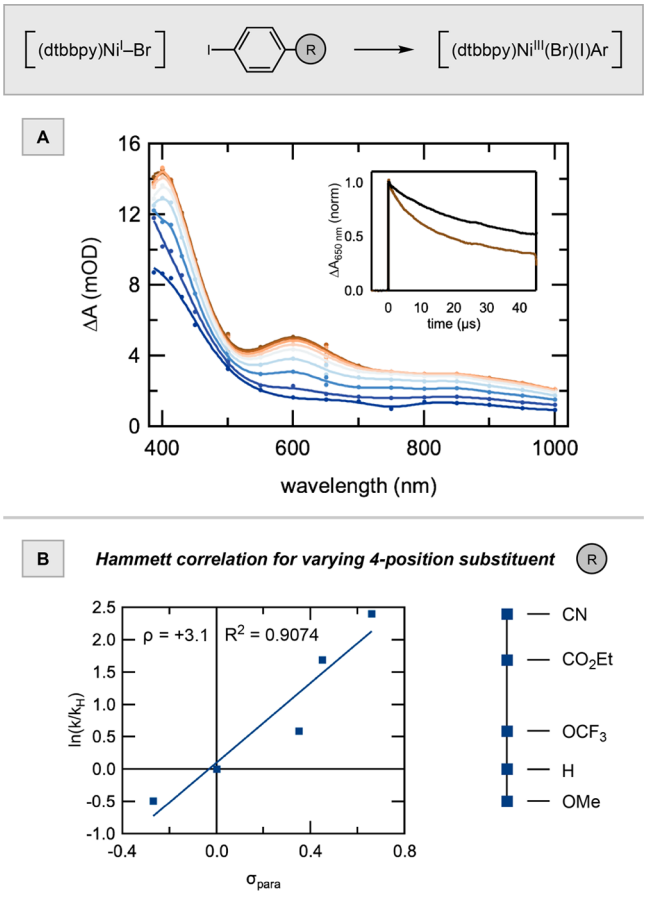

Figure 4. Spectral evolution for Ni(I) signal in the presence of ethyl 4-iodobenzoate (500 mM) (A) and Hammett correlation demonstrating oxidative addition rate sensitivity to aryl iodide electronics (B).

cathodic wave represents a two-electron reduction event ($E_{p/2}[Ni^{II}/Ni^{0}]$ = −1.1 V vs SCE, Figure S33).[23,41] Under preparative electrocatalytic conditions, a Ni(II)/Ni(0) comproportionation step following the initial cathodic reduction has been proposed to generate a catalytically active Ni(I) intermediate relevant to C−N cross-coupling.[23] Additionally, this elementary comproportionation step has been proposed in the context of Ni-catalyzed C−SCF$_3$ coupling.[42] With these studies in mind, we recognized that pulse radiolysis provided an opportunity to selectively generate single-electron-reduced [(dtbbpy)NiBr], as the pulsed electron beam generates a low total concentration of solvated electrons (∼1 μM).[37] Meanwhile, spectroelectrochemical investigation of [(dtbbpy)NiBr$_2$] reduction would enable spectroscopic measurement of the bulk electrolysis products relevant to the electrocatalytic setting. When irradiated in a manner analogous to that described previously, [(dtbbpy)NiBr$_2$] reduction produces a long-lived three-peaked signal with ΔA maxima at 430, 620, and 860 nm (Figure 3A). When [(dtbbpy)NiBr$_2$] reduction was monitored spectroelectrochemically, the resulting ΔA spectrum matched well with the pulse radiolysis data (Figure 3B), indicating that indeed Ni(0)/Ni(II) comproportionation to produce [(dtbbpy)NiBr] is rapid under synthetically relevant electrolysis conditions (Figure 3C). This finding holds implications for Ni-catalyzed cross-coupling processes, as the relevant nickel catalyst oxidation state can have a dramatic impact on feasible elementary organometallic steps.[1,12] Moreover, this experimental approach provides a method to interrogate the effects that additives in specific Ni-catalyzed reactions have on Ni(0)/Ni(II) comproportionation.

We next turned our attention to investigating the reactivity of [(dtbbpy)NiBr] generated through electrolysis and pulse radiolysis. Oxidative addition between reductively generated bipyridine-ligated Ni(I) intermediates and aryl halides is a commonly invoked elementary step across many nickel-catalyzed arylation reactions.[12] While the use of cyclic voltammetry and spectroelectrochemistry can provide some insight into this step, the two-electron nature of [(dtbbpy)-NiBr$_2$] cathodic reduction complicates the interpretation of these results. Nonetheless, reductive generation of low-valent dtbbpy-ligated nickel was carried out in the presence of 4-bromobenzotrifluoride, and its subsequent oxidative addition could be monitored by cyclic voltammetry and UV−vis absorption measurements (Figures S1−S4). Unfortunately, the possibility of [(dtbbpy)Ni] aryl halide oxidative addition competing with Ni(0)/Ni(II) comproportionation to generate [(dtbbpy)NiBr] makes it challenging to assign this reactivity to a Ni(0)/Ni(II) or Ni(I)/Ni(III) oxidative addition process (SI, page S5). Pulse radiolysis was then employed to directly probe the rate of aryl halide oxidative addition with [(dtbbpy)NiBr]. Examining the reactivity of 4-bromobenzotrifluoride with [(dtbbpy)NiBr] revealed no significant lifetime change in the Ni(I) signal by pulse radiolysis, providing an upper limit on the oxidative addition rate (k_{OA} < 10^4 M^{-1} s^{-1}, Figures S7 and S8). However, moving to the more reactive ethyl 4-iodobenzoate showed significant quenching of the Ni(I) signal (k_{OA} = 1.18 (±0.05) × 10^5 M^{-1} s^{-1}, Figure 4A), consistent with previously measured rate constants for Ni(I) aryl iodide oxidative addition.[17] To ensure efficient Ni(I) generation in quenching experiments involving high concentrations of aryl iodide, 1,3-dicyanobenzene (500 mM) was included as an electron-transfer mediator (see SI, page S12, for details). Rapid initial decay of the 620 nm [(dtbbpy)NiBr] signal leaves behind a long-lived spectrum which can be tentatively assigned to the corresponding Ni(III) aryl oxidative addition adduct (see SI, page S20, for discussion and Figure S16 for Ni(I) data without aryl iodide, showing no spectral evolution on the same time scale).

In order to probe the sensitivity of the Ni(I) oxidative addition rate to substrate electronics, a panel of electronically differentiated aryl iodides were examined by pulse radiolysis. Ni(I) signal decay kinetics were measured in the presence of up to 1000 mM 4-iodoanisole, iodobenzene, 4-(trifluoromethoxy)iodobenzene, ethyl 4-iodobenzoate, or 4-iodobenzonitrile. A plot of $\ln(k_{OA}/k_{OA}(H))$ vs σ_p for the corresponding 4-substituted iodoarenes reveals a strong dependence of the oxidative addition rate on arene electronics (ρ = +3.1, Figure 4B), with an 18-fold increase in rate over the studied range (σ = −0.27 to +0.66). The rapid reaction of iodobenzene with [(dtbbpy)NiBr] is of particular note, as the corresponding chloro-bridged dimer [(dtbbpy)NiCl]$_2$ was recently shown by Hazari and co-workers to be unreactive toward iodobenzene oxidative addition.[32]

In order to assess the influence of dimer formation on the rate of oxidative addition by [(dtbbpy)NiBr], [(dtbbpy)NiBr]$_2$ was independently synthesized, exposed to iodobenzene, and monitored by ^{1}H NMR analysis (Figure S38). Consistent with results obtained by Hazari and co-workers for the chloro-variant,[32] [(dtbbpy)NiBr]$_2$ shows no reactivity toward iodobenzene at room temperature up to 16 h. This reactivity

https://doi.org/10.1021/jacs.1c04652
J. Am. Chem. Soc. XXXX, XXX, XXX−XXX

contrasts dramatically with the rate measured for the monomeric form by pulse radiolysis (k_{OA} = 2.2 (±0.3) × 10^4 M^{-1} s^{-1}, Figure 5). Spectroelectrochemical measurements

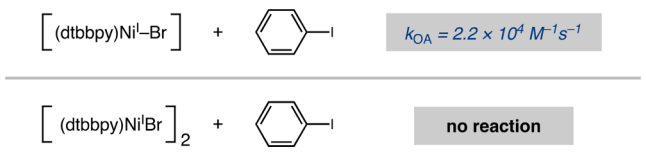

Figure 5. Relative rates of oxidative addition with iodobenzene for monomeric and dimeric bipyridine-ligated Ni(I)Br.

(Figure S9) show that [(dtbbpy)NiBr] dimerization occurs no faster than the minute time scale at catalytically relevant nickel concentrations. Together, these results indicate the importance of considering the immediate reduction products of nickel precatalysts in addition to complexes which may be thermodynamically favored.

To quantitatively assess the barrier to Ni(I) aryl iodide oxidative addition, Ni(I) quenching studies were carried out at various temperatures. Following the method of Eyring, a plot of $\ln(k_{OA}/T)$ vs $1/T$ was used to determine the enthalpic ($\Delta H^{\ddagger}$ = 5.8 ± 0.2 kcal·mol^{-1}) and entropic ($\Delta S^{\ddagger}$ = −15.5 ± 0.3 cal·mol^{-1}·K^{-1}) contributions to the overall reaction barrier ($\Delta G^{\ddagger}_{298\ K}$ = 10.4 ± 0.4 kcal·mol^{-1}, Figure 6). This data may

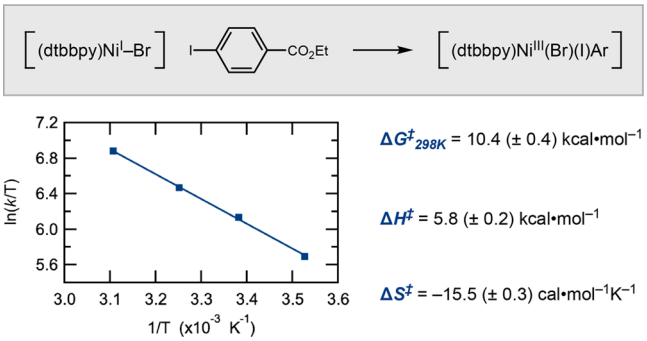

Figure 6. Eyring analysis of the oxidative addition between [(dtbbpy)NiBr] and ethyl 4-iodobenzoate.

serve as a useful experimental benchmark for computational investigations of Ni/photoredox-based cross-coupling reactions which have primarily relied on DFT-based oxidative addition barrier heights.[43−45]

The combined use of pulse radiolysis and spectroelectrochemistry has provided insights into fundamental elementary steps relevant to low-valent Ni intermediates commonly encountered in Ni-catalyzed cross-coupling reactions (Figure 7). The finding that Ni(0)/Ni(II) comproportionation to

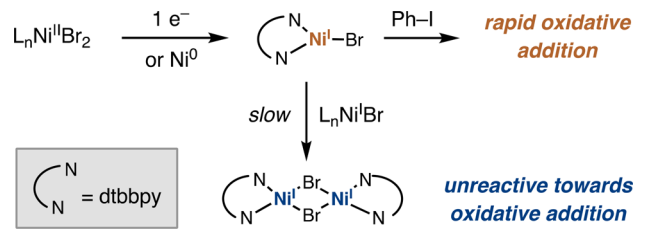

Figure 7. Overview of mechanisms for [(dtbbpy)NiBr] generation and reactivity.

generate bipyridine-ligated Ni(I) is rapid under synthetically relevant conditions holds relevance to the overall mechanism of multiple Ni-catalyzed C−C and C−X (X = N, O) cross-coupling reactions. Additionally, the investigation of Ni(I) oxidative addition by pulse radiolysis revealed the influence of aryl halide electronics on Ni(I) oxidative addition rates and the profound impact that dimer formation has on this elementary step. In particular, transiently generated [(dtbbpy)NiBr] rapidly reacts with iodobenzene, while the dimeric form, $[(dtbbpy)NiBr]_2$, is virtually unreactive. This information is especially relevant to reactions wherein high concentrations of low-valent Ni are thought to be deleterious, given the kinetic favorability of dimer formation under such conditions.[46] Taken together, these studies have important implications for reaction design in the area of Ni-catalyzed cross-coupling. More broadly, pulse radiolysis has been demonstrated to serve as a powerful tool for interrogating short-lived catalytic intermediates and measuring fast radical-based reactions relevant to photoredox and electrocatalysis cross-coupling platforms.

■ ASSOCIATED CONTENT

Supporting Information

The Supporting Information is available free of charge at https://pubs.acs.org/doi/10.1021/jacs.1c04652.

Experimental procedures, spectroscopic and electroanalytical data, and further discussions (PDF)

■ AUTHOR INFORMATION

Corresponding Authors

Matthew J. Bird − *Chemistry Division, Brookhaven National Laboratory, Upton, New York 11973, United States;* orcid.org/0000-0002-6819-5380; Email: mbird@bnl.gov

David W. C. MacMillan − *Merck Center for Catalysis, Princeton University, Princeton, New Jersey 08544, United States;* orcid.org/0000-0001-6447-0587; Email: dmacmill@princeton.edu

Authors

Nicholas A. Till − *Merck Center for Catalysis, Princeton University, Princeton, New Jersey 08544, United States;* orcid.org/0000-0003-2421-7186

Seokjoon Oh − *Chemistry Division, Brookhaven National Laboratory, Upton, New York 11973, United States;* orcid.org/0000-0002-8980-5213

Complete contact information is available at: https://pubs.acs.org/10.1021/jacs.1c04652

Notes

The authors declare no competing financial interest.

■ ACKNOWLEDGMENTS

N.A.T., S.O., D.W.C.M., and M.B. acknowledge support from BioLEC, an Energy Frontier Research Center funded by the U.S. Department of Energy, Office of Science, Basic Energy Sciences, under Award DE-SC0019370. Use of the Laser Electron Accelerator Facility (LEAF) of the BNL Accelerator Center for Energy Research (ACER) was supported by U.S. Department of Energy, Office of Science, Office of Basic Energy Sciences, Division of Chemical Sciences, Geosciences & Bioscience, through contract DE-SC0012704.

https://doi.org/10.1021/jacs.1c04652
J. Am. Chem. Soc. XXXX, XXX, XXX−XXX

REFERENCES

(1) Tasker, S. Z.; Standley, E. A.; Jamison, T. F. Recent Advances in Homogeneous Nickel Catalysis. *Nature* **2014**, *509* (7500), 299−309.

(2) Milligan, J. A.; Phelan, J. P.; Badir, S. O.; Molander, G. A. Alkyl Carbon−Carbon Bond Formation by Nickel/Photoredox Cross-Coupling. *Angew. Chem., Int. Ed.* **2019**, *58* (19), 6152−6163.

(3) Twilton, J.; Le, C.; Zhang, P.; Shaw, M. H.; Evans, R. W.; MacMillan, D. W. C. The Merger of Transition Metal and Photocatalysis. *Nature Reviews Chemistry* **2017**, *1* (7), 0052.

(4) Levin, M. D.; Kim, S.; Toste, F. D. Photoredox Catalysis Unlocks Single-Electron Elementary Steps in Transition Metal Catalyzed Cross-Coupling. *ACS Cent. Sci.* **2016**, *2* (5), 293−301.

(5) Zhu, C.; Yue, H.; Chu, L.; Rueping, M. Recent Advances in Photoredox and Nickel Dual-Catalyzed Cascade Reactions: Pushing the Boundaries of Complexity. *Chemical Science* **2020**, *11* (16), 4051−4064.

(6) Li, C.; Kawamata, Y.; Nakamura, H.; Vantourout, J. C.; Liu, Z.; Hou, Q.; Bao, D.; Starr, J. T.; Chen, J.; Yan, M.; Baran, P. S. Electrochemically Enabled, Nickel-Catalyzed Amination. *Angew. Chem., Int. Ed.* **2017**, *56* (42), 13088−13093.

(7) Truesdell, B. L.; Hamby, T. B.; Sevov, C. S. General C(Sp2)−C(Sp3) Cross-Electrophile Coupling Reactions Enabled by Overcharge Protection of Homogeneous Electrocatalysts. *J. Am. Chem. Soc.* **2020**, *142* (12), 5884−5893.

(8) Lu, J.; Wang, Y.; McCallum, T.; Fu, N. Harnessing Radical Chemistry via Electrochemical Transition Metal Catalysis. *iScience* **2020**, *23* (12), 101796.

(9) Gu, J.; Wang, X.; Xue, W.; Gong, H. Nickel-Catalyzed Reductive Coupling of Alkyl Halides with Other Electrophiles: Concept and Mechanistic Considerations. *Org. Chem. Front.* **2015**, *2* (10), 1411−1421.

(10) Dombrowski, A. W.; Gesmundo, N. J.; Aguirre, A. L.; Sarris, K. A.; Young, J. M.; Bogdan, A. R.; Martin, M. C.; Gedeon, S.; Wang, Y. Expanding the Medicinal Chemist Toolbox: Comparing Seven C(Sp2)−C(Sp3) Cross-Coupling Methods by Library Synthesis. *ACS Med. Chem. Lett.* **2020**, *11* (4), 597−604.

(11) Zhang, R.; Li, G.; Wismer, M.; Vachal, P.; Colletti, S. L.; Shi, Z.-C. Profiling and Application of Photoredox C(Sp3)−C(Sp2) Cross-Coupling in Medicinal Chemistry. *ACS Med. Chem. Lett.* **2018**, *9* (7), 773−777.

(12) Diccianni, J. B.; Diao, T. Mechanisms of Nickel-Catalyzed Cross-Coupling Reactions. *TRECHEM* **2019**, *1* (9), 830−844.

(13) Zuo, Z.; Ahneman, D. T.; Chu, L.; Terrett, J. A.; Doyle, A. G.; MacMillan, D. W. C. Merging Photoredox with Nickel Catalysis: Coupling of α-Carboxyl Sp3-Carbons with Aryl Halides. *Science* **2014**, *345* (6195), 437−440.

(14) Tellis, J. C.; Primer, D. N.; Molander, G. A. Single-Electron Transmetalation in Organoboron Cross-Coupling by Photoredox/Nickel Dual Catalysis. *Science* **2014**, *345* (6195), 433−436.

(15) Kudisch, M.; Lim, C.-H.; Thordarson, P.; Miyake, G. M. Energy Transfer to Ni-Amine Complexes in Dual Catalytic, Light-Driven C−N Cross-Coupling Reactions. *J. Am. Chem. Soc.* **2019**, *141* (49), 19479−19486.

(16) Sun, R.; Qin, Y.; Ruccolo, S.; Schnedermann, C.; Costentin, C.; Nocera, D. G. Elucidation of a Redox-Mediated Reaction Cycle for Nickel-Catalyzed Cross Coupling. *J. Am. Chem. Soc.* **2019**, *141* (1), 89−93.

(17) Qin, Y.; Sun, R.; Gianoulis, N. P.; Nocera, D. G. Photoredox Nickel-Catalyzed C−S Cross-Coupling: Mechanism, Kinetics, and Generalization. *J. Am. Chem. Soc.* **2021**, *143* (4), 2005−2015.

(18) Tian, L.; Till, N. A.; Kudisch, B.; MacMillan, D. W. C.; Scholes, G. D. Transient Absorption Spectroscopy Offers Mechanistic Insights for an Iridium/Nickel-Catalyzed C−O Coupling. *J. Am. Chem. Soc.* **2020**, *142* (10), 4555−4559.

(19) Till, N. A.; Tian, L.; Dong, Z.; Scholes, G. D.; MacMillan, D. W. C. Mechanistic Analysis of Metallaphotoredox C−N Coupling: Photocatalysis Initiates and Perpetuates Ni(I)/Ni(III) Coupling Activity. *J. Am. Chem. Soc.* **2020**, *142* (37), 15830−15841.

(20) Ting, S. I.; Garakyaraghi, S.; Taliaferro, C. M.; Shields, B. J.; Scholes, G. D.; Castellano, F. N.; Doyle, A. G. 3d-d Excited States of Ni(II) Complexes Relevant to Photoredox Catalysis: Spectroscopic Identification and Mechanistic Implications. *J. Am. Chem. Soc.* **2020**, *142* (12), 5800−5810.

(21) Arias-Rotondo, D. M.; McCusker, J. K. The Photophysics of Photoredox Catalysis: A Roadmap for Catalyst Design. *Chem. Soc. Rev.* **2016**, *45* (21), 5803−5820.

(22) Sandford, C.; Edwards, M. A.; Klunder, K. J.; Hickey, D. P.; Li, M.; Barman, K.; Sigman, M. S.; White, H. S.; Minteer, S. D. A Synthetic Chemist's Guide to Electroanalytical Tools for Studying Reaction Mechanisms. *Chem. Sci.* **2019**, *10* (26), 6404−6422.

(23) Kawamata, Y.; Vantourout, J. C.; Hickey, D. P.; Bai, P.; Chen, L.; Hou, Q.; Qiao, W.; Barman, K.; Edwards, M. A.; Garrido-Castro, A. F.; deGruyter, J. N.; Nakamura, H.; Knouse, K.; Qin, C.; Clay, K. J.; Bao, D.; Li, C.; Starr, J. T.; Garcia-Irizarry, C.; Sach, N.; White, H. S.; Neurock, M.; Minteer, S. D.; Baran, P. S. Electrochemically Driven, Ni-Catalyzed Aryl Amination: Scope, Mechanism, and Applications. *J. Am. Chem. Soc.* **2019**, *141* (15), 6392−6402.

(24) Hickey, D. P.; Sandford, C.; Rhodes, Z.; Gensch, T.; Fries, L. R.; Sigman, M. S.; Minteer, S. D. Investigating the Role of Ligand Electronics on Stabilizing Electrocatalytically Relevant Low-Valent Co(I) Intermediates. *J. Am. Chem. Soc.* **2019**, *141* (3), 1382−1392.

(25) Siu, J. C.; Sauer, G. S.; Saha, A.; Macey, R. L.; Fu, N.; Chauviré, T.; Lancaster, K. M.; Lin, S. Electrochemical Azidooxygenation of Alkenes Mediated by a TEMPO−N3 Charge-Transfer Complex. *J. Am. Chem. Soc.* **2018**, *140* (39), 12511−12520.

(26) Schley, N. D.; Fu, G. C. Nickel-Catalyzed Negishi Arylations of Propargylic Bromides: A Mechanistic Investigation. *J. Am. Chem. Soc.* **2014**, *136* (47), 16588−16593.

(27) Lin, Q.; Diao, T. Mechanism of Ni-Catalyzed Reductive 1,2-Dicarbofunctionalization of Alkenes. *J. Am. Chem. Soc.* **2019**, *141* (44), 17937−17948.

(28) Biswas, S.; Weix, D. J. Mechanism and Selectivity in Nickel-Catalyzed Cross-Electrophile Coupling of Aryl Halides with Alkyl Halides. *J. Am. Chem. Soc.* **2013**, *135* (43), 16192−16197.

(29) Zarate, C.; Yang, H.; Bezdek, M. J.; Hesk, D.; Chirik, P. J. Ni(I)−X Complexes Bearing a Bulky α-Diimine Ligand: Synthesis, Structure, and Superior Catalytic Performance in the Hydrogen Isotope Exchange in Pharmaceuticals. *J. Am. Chem. Soc.* **2019**, *141* (12), 5034−5044.

(30) Somerville, R. J.; Odena, C.; Obst, M. F.; Hazari, N.; Hopmann, K. H.; Martin, R. Ni(I)−Alkyl Complexes Bearing Phenanthroline Ligands: Experimental Evidence for CO2 Insertion at Ni(I) Centers. *J. Am. Chem. Soc.* **2020**, *142* (25), 10936−10941.

(31) Wagner, C. L.; Herrera, G.; Lin, Q.; Hu, C. T.; Diao, T. Redox Activity of Pyridine-Oxazoline Ligands in the Stabilization of Low-Valent Organonickel Radical Complexes. *J. Am. Chem. Soc.* **2021**, *143* (14), 5295−5300.

(32) Mohadjer Beromi, M.; Brudvig, G. W.; Hazari, N.; Lant, H. M. C.; Mercado, B. Q. Synthesis and Reactivity of Paramagnetic Nickel Polypyridyl Complexes Relevant to C(Sp2)−C(Sp3)Coupling Reactions. *Angew. Chem., Int. Ed.* **2019**, *58* (18), 6094−6098.

(33) Masarwa, A.; Meyerstein, D. Properties of Transition Metal Complexes with Metal−Carbon Bonds in Aqueous Solutions As Studied by Pulse Radiolysis. In *Advances in Inorganic Chemistry*, Including Bioinorganic Studies; van Eldik, R., Ed.; Academic Press, 2004; Vol. 55, pp 271−313. DOI: 10.1016/S0898-8838(03)55005-X.

(34) Grills, D. C.; Polyansky, D. E.; Fujita, E. Application of Pulse Radiolysis to Mechanistic Investigations of Catalysis Relevant to Artificial Photosynthesis. *ChemSusChem* **2017**, *10* (22), 4359−4373.

(35) Kobayashi, K. Pulse Radiolysis Studies for Mechanism in Biochemical Redox Reactions. *Chem. Rev.* **2019**, *119* (6), 4413−4462.

(36) Miller, J. R.; Calcaterra, L. T.; Closs, G. L. Intramolecular Long-Distance Electron Transfer in Radical Anions. The Effects of Free Energy and Solvent on the Reaction Rates. *J. Am. Chem. Soc.* **1984**, *106* (10), 3047−3049.

https://doi.org/10.1021/jacs.1c04652
J. Am. Chem. Soc. XXXX, XXX, XXX−XXX

(37) Wishart, J. F.; Cook, A. R.; Miller, J. R. The LEAF Picosecond Pulse Radiolysis Facility at Brookhaven National Laboratory. *Rev. Sci. Instrum.* **2004**, *75* (11), 4359−4366.
(38) Ciszewski, J. T.; Mikhaylov, D. Y.; Holin, K. V.; Kadirov, M. K.; Budnikova, Y. H.; Sinyashin, O.; Vicic, D. A. Redox Trends in Terpyridine Nickel Complexes. *Inorg. Chem.* **2011**, *50* (17), 8630−8635.
(39) Budnikova, Y. H.; Vicic, D. A.; Klein, A. Exploring Mechanisms in Ni Terpyridine Catalyzed C−C Cross-Coupling Reactions—A Review. *Inorganics* **2018**, *6* (1), 18.
(40) Hayon, E.; Hayashi, N.; Ibata, T.; Lichtin, N. N.; Matsumoto, A. Pulse Radiolysis of Liquid Amides. *J. Phys. Chem.* **1971**, *75* (15), 2267−2272.
(41) Amatore, C.; Azzabi, M.; Calas, P.; Jutand, A.; Lefrou, C.; Rollin, Y. Absolute Determination of Electron Consumption in Transient or Steady State Electrochemical Techniques. *J. Electroanal. Chem. Interfacial Electrochem.* **1990**, *288* (1), 45−63.
(42) Kalvet, I.; Guo, Q.; Tizzard, G. J.; Schoenebeck, F. When Weaker Can Be Tougher: The Role of Oxidation State (I) in P- vs N-Ligand-Derived Ni-Catalyzed Trifluoromethylthiolation of Aryl Halides. *ACS Catal.* **2017**, *7* (3), 2126−2132.
(43) Gutierrez, O.; Tellis, J. C.; Primer, D. N.; Molander, G. A.; Kozlowski, M. C. Nickel-Catalyzed Cross-Coupling of Photoredox-Generated Radicals: Uncovering a General Manifold for Stereoconvergence in Nickel-Catalyzed Cross-Couplings. *J. Am. Chem. Soc.* **2015**, *137* (15), 4896−4899.
(44) Yuan, M.; Song, Z.; Badir, S. O.; Molander, G. A.; Gutierrez, O. On the Nature of C(Sp3)−C(Sp2) Bond Formation in Nickel-Catalyzed Tertiary Radical Cross-Couplings: A Case Study of Ni/Photoredox Catalytic Cross-Coupling of Alkyl Radicals and Aryl Halides. *J. Am. Chem. Soc.* **2020**, *142* (15), 7225−7234.
(45) Maity, B.; Zhu, C.; Yue, H.; Huang, L.; Harb, M.; Minenkov, Y.; Rueping, M.; Cavallo, L. Mechanistic Insight into the Photoredox-Nickel-HAT Triple Catalyzed Arylation and Alkylation of α-Amino Csp3−H Bonds. *J. Am. Chem. Soc.* **2020**, *142* (40), 16942−16952.
(46) Gisbertz, S.; Reischauer, S.; Pieber, B. Overcoming Limitations in Dual Photoredox/Nickel-Catalysed C−N Cross-Couplings Due to Catalyst Deactivation. *Nature Catalysis* **2020**, *3* (8), 611−620.

https://doi.org/10.1021/jacs.1c04652
J. Am. Chem. Soc. XXXX, XXX, XXX−XXX